Molecular Biology of the Cell
Vol. 11, 2605–2616, August 2000

The Yeast *TEL1* Gene Partially Substitutes for Human *ATM* in Suppressing Hyperrecombination, Radiation-Induced Apoptosis and Telomere Shortening in A-T Cells

Eberhard Fritz,[*‖] Anna A. Friedl,[†] Ralf M. Zwacka,[‡] Friederike Eckardt-Schupp,[*] and M. Stephen Meyn[§]

[*]GSF, National Research Center for Environment and Health, Institute of Radiobiology, 85758 Neuherberg, Germany [†]Department of Radiobiology, University of Munich, 80336 Munich, Germany [‡]University of Edinburgh, Department of Oncology, Edinburgh, United Kingdom [§]The Hospital for Sick Children, Toronto M5G 1X8, Canada

Submitted December 27, 1999; Revised May 8, 2000; Accepted June 12, 2000
Monitoring Editor: Alan P. Wolffe

Homozygous mutations in the human *ATM* gene lead to a pleiotropic clinical phenotype of ataxia-telangiectasia (A-T) patients and correlating cellular deficiencies in cells derived from A-T donors. *Saccharomyces cerevisiae tel1* mutants lacking Tel1p, which is the closest sequence homologue to the ATM protein, share some of the cellular defects with A-T. Through genetic complementation of A-T cells with the yeast *TEL1* gene, we provide evidence that Tel1p can partially compensate for ATM in suppressing hyperrecombination, radiation-induced apoptosis, and telomere shortening. Complementation appears to be independent of p53 activation. The data provided suggest that *TEL1* is a functional homologue of human *ATM* in yeast, and they help to elucidate different cellular and biochemical pathways in human cells regulated by the ATM protein.

INTRODUCTION

Ataxia-telangiectasia (A-T) is an autosomal recessive disorder characterized by a pleiotropic clinical phenotype that includes cerebellar degeneration, radiation hypersensitivity, immunodeficiency, genomic instability, premature aging, and a high cancer risk (Lavin and Shiloh, 1997; Shiloh, 1997; Gatti, 1998; Meyn, 1999). A-T is caused by functional inactivation of the *ATM* gene on 11q23 (Gatti *et al.*, 1988; Savitsky *et al.*, 1995a). Typical A-T patients are compound heterozygotes for *ATM* mutations that result in complete loss of detectable protein (Lakin *et al.*, 1996), while mutations with less severe effects on ATM expression and function can cause milder phenotypes (Gilad *et al.*, 1996; Meyn, 1999). Cultured A-T cells lack radiation-induced cell cycle checkpoints and express cellular defects that correlate with the clinical phenotype (see Meyn, 1995); e.g., the sensitivity of A-T patients to ionizing radiation (IR) is reflected by reduced clonogenic survival and increased apoptosis of cultured A-T cells following exposure to IR (Meyn *et al.*, 1994; Taylor *et al.*, 1994; Duchaud *et al.*, 1996). The in vivo chromosomal instability is paralleled by increased numbers of chromosome aberrations (Aurias *et al.*, 1980; Carney, 1999) and high rates of spontaneous recombination in A-T cells grown in culture (Meyn, 1993; Luo *et al.*, 1996). Symptoms of premature aging in A-T patients correlate with early senescence and accelerated telomere shortening in cultured A-T fibroblasts (Pandita *et al.*, 1995; Metcalfe *et al.*, 1996; Xia *et al.*, 1996; Vaziri *et al.*, 1997).

Based on the phenotypic deficiencies of A-T patients, $Atm^{-/-}$ mice, and $Atm^{-/-}$ cells, and according to initial analyses of ATM protein interactions and catalytic activity, it is assumed that ATM is a key early component of a protein kinase cascade that activates multiple signaling pathways after the induction of double-strand breaks in DNA (DSBs) (Rotman and Shiloh, 1998; Meyn, 1999). In addition to its role in mediating cellular responses to DSBs, ATM also may be involved in other cellular stress responses (Rotman and Shiloh, 1998).

The proposed functional role of ATM is supported by structural analysis. Based on sequence homology, ATM belongs to a family of large eukaryotic proteins that regulate cellular responses to DNA damage, including DNA repair,

‖Corresponding author. E-mail address: efritz@gsf.de.
Abbreviations used: A-T, ataxia-telangiectasia; IR, ionizing radiation; PI3K, phosphatidyl-inositol-3-kinase; SV40, simian virus 40; TRF, terminal restriction fragment

genetic recombination, apoptosis, and cell cycle checkpoints (Keith and Schreiber, 1995; Savitsky *et al.*, 1995b; Hoekstra, 1997). The homology between these proteins is greatest in their carboxy terminal kinase domains. Although these regions are similar to the kinase domains of PI3 lipid kinases, ATM and several of its homologues express protein kinase activities in vitro (Keegan *et al.*, 1996).

The *Saccharomyces cerevisiae* protein Tel1p is the closest known sequence homologue to ATM, sharing 45% amino acid identity in the kinase domain and 21% amino acid identity in the rest of the protein (Greenwell *et al.*, 1995; Morrow *et al.*, 1995). There also are functional similarities between the two proteins. Both are required for phosphorylation of downstream proteins following DNA damage. IR-induced phosphorylation of p53, c-abl, and Rad51 in human cells is ATM dependent (Baskaran *et al.*, 1997; Shafman *et al.*, 1997; Banin *et al.*, 1998; Canman *et al.*, 1998; Kharbanda *et al.*, 1998; Yuan *et al.*, 1998), and *TEL1* controls damage-induced phosphorylation of Rfa2p, Rad53p, and Rad9p in yeast (Brush *et al.*, 1996; Sugimoto *et al.*, 1997; Emili, 1998; Vialard *et al.*, 1998). *TEL1*-deficient yeast cells express an A-T like genome instability that includes chromosome loss, hyperrecombination, and telomere shortening (Lustig and Petes, 1986; Greenwell *et al.*, 1995). In addition, *TEL1* may cooperate with another ATM homologue, *MEC1*, to provide ATM-like functions in yeast, since *tel1/mec1* double mutants show synergistic hypersensitivity to DNA damage, and expression of an extra copy of *TEL1* can rescue the lethality of *mec1* null mutants and can complement the hypersensitivity of *mec1* mutants to DNA damage (Morrow *et al.*, 1995). Taken together, these findings have led to the hypothesis that Tel1p may be a functional homologue of ATM and prompted us to analyze functional properties shared between these two proteins. We specifically asked whether expression of the yeast *TEL1* gene in human cells lacking ATM protein can complement their A-T phenotype.

We now provide evidence that expression of the yeast *TEL1* gene in A-T cells partially suppresses a specific subset of cellular A-T deficiencies: hyperrecombination, IR-induced apoptosis, and telomere shortening. Our cross-complementation data suggest that Tel1p shares functional properties with ATM, and they help to elucidate distinct cellular pathways regulated by ATM. In addition, our results support the concept that human ATM is involved in regulating telomere length, perhaps in a similar manner to that of Tel1p in *S. cerevisiae*.

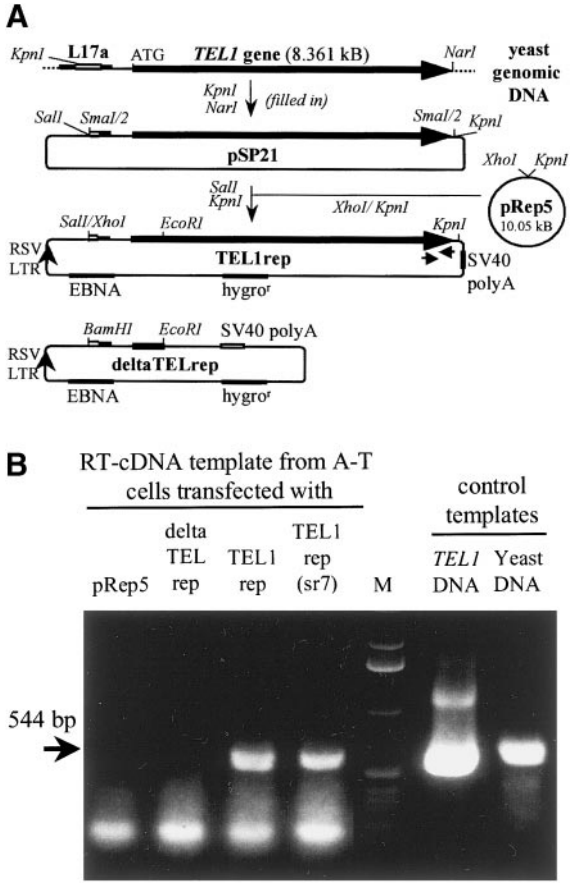

Figure 1. (A) Cloning of mammalian *TEL1* expression constructs. Genomic organization of the *TEL1* locus and construction of plasmid pSP21 was described by Greenwell *et al.* (1995). TEL1rep contains the complete *TEL1* gene (8361 bp) from *S. cerevisiae* cloned into the mammalian expression vector pRep5; deltaTELrep contains only the first 993 bp of *TEL1*. Both vectors include an unrelated genomic region upstream of the *TEL1* gene encoding parts of the ribosomal protein L17a. The location of PCR primers FOR3 and REV3 is indicated by arrows at the 3′ end of TEL1rep. (B) Detection of TEL1-RNA in TEL1rep-transfected A-T cells. Total RNA was extracted from stably transfected cell populations, DNAseI digested and reverse transcribed. PCR primers FOR3 (CTATCGTTGGATACATATTAGGCC) and REV3 (CCATCCCATATATATAACACTC) specifically amplified a 544-bp fragment in RT-cDNAs from a pooled A-T population stably transfected with the TEL1rep expression plasmid (TEL1rep) and a derived subclone, TEL1rep(sr7). Control templates include RT-cDNA from populations transfected with the empty vector (pRep5) and truncated vector (deltaTElrep) as well as *TEL1* DNA (TEL1rep) and yeast genomic DNA.

MATERIALS AND METHODS

Cloning of TEL1 Expression Constructs

The complete *TEL1* coding sequence (8361 bp), including 1138 bp upstream of *TEL1*, was excised from the pSP21 plasmid (Greenwell *et al.*, 1995) after digestion with *Sal*I and *Kpn*I and was ligated into the *Xho*I and *Kpn*I sites of the mammalian expression vector pRep5 (Groger *et al.*, 1989) (see Figure 1A). After gel purification of the expected ligation product, transformation of *Escherichia coli* DH5α yielded recombinant colonies that harbor the complete *TEL1* gene encoding 2787 amino acids in pRep5 (TEL1rep). The integrity of the *TEL1* insertion was confirmed by multiple restriction digests. The deltaTELrep vector was generated using a truncated *TEL1* version from the plasmid pPG40 (Greenwell, unpublished). After cutting pPG40 with *Kpn*I and *Eco*RI, and inserting the truncated 2130-bp *TEL1* fragment into the vector pRSET-B (Invitrogen, Carlsbad, CA), the insert was reexcised with *Bam*HI and partial *Hin*dIII digestion and was inserted into pRep5. The plasmid deltaTELrep thus covers the first 993 bp of *Tel1* encoding the first 331 amino acids. Both expression vectors contain an unrelated genomic region upstream of *TEL1* that includes a 315-bp intronic sequence connected to the second exon (369 bp) of the yeast ribosomal protein L17a (Leer *et al.*, 1984). Based on computer analysis, translation starting at internal ATG codons within the unrelated upstream L17a open reading frame could not lead to formation of a functional L17a protein of 137 amino acids but could result in production of N-terminally trun-

cated peptides consisting of 115, 82, 79, 65, or 29 amino acids. However, we can rule out the possibility that these truncated L17a peptides are responsible for the complementation seen with TEL1rep, since the upstream L17a region is also present in the deltaTELrep expression vector and the expression of deltaTELrep in A-T cells has no effect on the complementation of cellular phenotypes.

Cell Culture, Transfection, and Analysis of Radiation Sensitivity

Simian virus 40 (SV40)-immortalized A-T fibroblasts AT5BIVA (GM5849) and derivatives that contain a stably integrated pLrec recombination vector (5L13) were stably transfected with the expression vectors as described previously (Meyn *et al.*, 1993). Briefly, 8 μg of DNA were electroporated into 5×10^6 cells using a Bio-Rad (Hercules, CA) gene pulser (750 V, 25 μF, 200 Ohm, and 0.4 cm cuvettes), and cells were selected for stable uptake of expression plasmids by growth in 100 μg/ml hygromycin (Calbiochem, San Diego, CA) for 2–3 wk. Unless stated otherwise, phenotypic analyses were carried out using pools of stably transfected hyg^R colonies arising after each transfection rather than single clonal isolates. For some experiments, following transfection with *TEL1* or deltaTEL expression constructs, cell cultures were exposed to streptonigrin in a selection regimen (0.1 ng/ml, for 7 d) that allowed few nonresistant cells to survive. Individual subclones that were growing after exposure to streptonigrin were isolated. Analyses of cellular A-T phenotypes were routinely compared with the normal SV40-transformed fibroblast lines GM0639 and/or GM0847 (Lesch-Nyhan syndrome). γ-Irradiation was performed using a ^{137}Cs source (Mark I, model 68A, J. L. Shepherd & Associates, San Fernando, CA) at a dose rate of 2.29 Gy/min. Analyses of colony survival and radiation-induced apoptosis were performed as described before (Meyn *et al.*, 1994). Briefly, apoptotic cells were stained with a combination of 4′,6-diamidino-2-phenylindole (DAPI), calcein acetoxymethyl ester, and ethidium homodimer (Eth-D1) (all from Molecular Probes, Eugene, OR); were examined by fluorescence microscopy in a double-blind manner; and were scored as living, necrotic, or apoptotic based on their characteristic fluorescence pattern and morphology. In addition, apoptotic subG1 cells were scored after staining with propidium iodide in FACS analyses, as described elsewhere (Chen *et al.*, 1999).

RT-PCR

Total RNA was extracted from stably transfected cells using the PUREscript RNA isolation kit (Gentra Systems, Minneapolis, MN). Total RNA was treated overnight with 50 U of RNAse free DNAseI (Boehringer Mannheim, Mannheim, Germany) at 25°C to exclude false-positive PCR products due to residual genomic or plasmid DNA. Reverse transcription and PCR reactions were performed using standard protocols. PCR primers FOR3 (CTATCGTTGGATACATATTAGGCC) and REV3 (CCATCCCATATATATAACACTC) are located at the extreme 3′ end of the *TEL1* coding sequence (Figure 1A) and specifically amplified a 544-bp fragment ending 12 bp upstream of the stop codon.

Analyses of Telomere Length

Stably transfected cells were continuously cultured for 4 mo. Alternatively, cells were exposed to streptonigrin after 3 mo of cultivation, and the resulting clones were expanded; in both cases, genomic DNA was then repeatedly isolated during another 12 mo of further passaging using standard procedures. In addition, 20 random colonies emerging from single cells then were isolated from the pooled transfected populations. These subclones again were expanded, and genomic DNA was isolated for control experiments showing the clonal heterogeneity of the pooled population. After complete digestion with *Hin*fI and/or *Alu*I, the genomic DNA was separated by 0.8% agarose gel electrophoresis (80 V, 6 h), was transferred to nylon membrane (Qiagen, Hilden, Germany), and was hybridized to P^{32}-labeled probes of high molecular size telomeric repeats according to the manufacturer's protocol. The telomeric probe was generated in a template-free PCR by staggered annealing of telomere-oligonucleotides TEL1/2 $(TTAGGG)_5$ and TEL2/2 $(CCCTAA)_5$ using P^{32}-dCTP in the nucleotide mix (Ijdo *et al.*, 1991), which yielded double-stranded (TTAGGG/AATCCC)n repetitive fragments of up to 10 kBp length. The high molecular size telomeric amplification products were purified using the PCR purification kit (Qiagen). The sequence specificity of the telomeric repeats was confirmed by fluorescence in situ hybridization of telomeres in metaphase spreads from human fibroblasts using telomeric amplification products that had subsequently been biotinylated (data not shown). Following autoradiography, smears of terminal restriction fragments (TRFs) were detected by the telomeric probe. Films were scanned with a GTZ 9000 scanner (Epson, Torrance, CA), and hybridization signals were analyzed using the RFLPscan software from Scanalytics (Billerica, MA). The mean TRF length was estimated by determining the mode of the optical density distribution on the autoradiographs (Oexle, 1998), and the size of fragments giving the peak intensity of the Gaussian-distributed TRF signals was calculated after comparison to the size standards.

Determination of Intrachromosomal Recombination Rates

Spontaneous intrachromosomal recombination after transfection of the *TEL1* expression constructs was measured in fluctuation analyses as described previously (Meyn, 1993). Briefly, the AT5BIVA derivative cell line 5L13 contains one chromosomally integrated copy of the pLrec recombination vector. pLrec encodes two different mutant alleles of the *lacZ* gene that can be converted to a functional $lacZ^+$ gene upon intrachromosomal recombination. $LacZ^+$ cells are visualized upon histochemical staining that detects the encoded β-GAL activity. Recombination rates were calculated using tables for the estimation of spontaneous mutation rates according to Luria & Delbrück (Capizzi and Jameson, 1972).

In an alternative protocol, 5L13 cells were freshly transfected with the *TEL1* expression constructs. Following transfection, cells were grown in hygromycin to select for those cells that had been stably transformed with the *TEL1* vectors. At 16 d, the resultant hyg^R colonies were stained histochemically for β-GAL expresssion. A few colonies from each transfection contained blue cells expressing β-GAL as a result of a spontaneous intrachromosomal recombination event involving the integrated pLec vector. β-GAL-positive colonies were always mosaics, indicating that they were not arising from cells that recombined their pLrec sequences before transfection. Instead, the mosaicism indicates that the observed pLrec recombination events took place after transfection with the *TEL1* expression constructs. Colonies containing recombination-positive cells ($lacZ^+$) were counted, and the colony conversion frequency determined after counterstaining and counting the total number of colonies.

Western Analyses and Electrophoretic Mobility Shift Assays

Nuclear extracts were prepared from transfected A-T cells and normal GM637 cells that had been grown on 150 mm plates. Following treatment with IR, the subconfluent cells were washed twice with ice-cold PBS and then were harvested with a rubber policeman in 1 ml of PBS. The cells were pelleted in a microfuge at 1500 rpm for 5 min at 4°C. After resuspending the cells in 600 μl of Dignam A buffer (10 mM HEPES [pH 7.9], 1.5 mM $MgCl_2$, 10 mM KCl, 1 mM DTT, and 1 mM PMSF), they were incubated on ice for 15 min. In order to lyse the cells, they were passed five times through a 25-gauge needle. Subsequently the nuclei were pelleted by centrifugation at 14,000 rpm for 1 min at 4°C. The nuclei were resus-

pended in 300 μl of Dignam C buffer (20 mM HEPES [pH 7.9], 25% glycerol, 0.42 mM NaCl, 1.5 mM $MgCl_2$, 0.2 mM EDTA, 1 mM DTT, and 1 mM PMSF) and were incubated for 30 min at 4°C with gentle agitation. The membranes then were pelleted, and the supernatant was transferred to a new tube. A Bradford assay (Bio-Rad) was used to measure the protein content of the nuclear extracts, and the concentrations of all samples were adjusted to 1 μg/μl. For Western analyses, nuclear extracts (5 μg) from *TEL1*-transfected A-T cells and control GM637 cells were separated on a denaturing 10% SDS-PAGE and then were transferred to a PVDF membrane (Bio-Rad) for 30 min on a semidry electroblotter at 10 V. The membrane was stained with 0.5% PonceauS to check for efficient and equal transfer and subsequently was blocked in 4% nonfat dry milk solution in PBS, supplemented with 0.3% Tween 20. This solution was used for all other antibody incubations and washing steps. The primary anti-p53 antibody DO-1(Oncogene Science, Cambridge, MA) was diluted 1:1000 and was incubated for 1 h at room temperature (RT) after which the membrane was washed four times. The secondary antibody, an anti-mouse IgG conjugated to horseradish peroxidase (Amersham, Little Chalfont, UK), was used at a 1:2000 dilution and incubated for 1 h at RT. Signals were visualized using an enhanced chemiluminescence mix (ECL, Amersham) and subsequent exposure to x-ray film. For EMSAs, 3 μl of nuclear extract (1 μg/μl) were incubated for 30 min at RT with 3.4 μl of 5x EMSA buffer (250 mM KCl, 100 mM HEPES [pH 7.9], 25% glycerol, 5 mM EDTA, and 5 mM DTT), 1 μl BSA (1 μg/μl), 1 μl poly(dI-dC) oligo (1 μg/μl), 7.6 μl H_2O, and 2 μl of ^{32}P end-labeled double-stranded oligonucleotide carrying a p53 binding consensus sequence. The p53-oligo (5′-TAC AGA ACA TGT CTA AGC ATG CTG GGG ACT-3′) is identical to nucleotides 1572–1601 of the human GADD45 gene (Kastan *et al.*, 1992). In supershift experiments, the mix was preincubated on ice for 2 h with 2 μl of anti-p53 monoclonal antibody (1 μg/μl, pAb 421, Oncogene Science). The mix was separated on a 4% native polyacrylamide gel, followed by drying and autoradiography.

RESULTS

TEL1 Is Expressed in A-T Cells upon Stable Transfection

In order to test expression of the yeast *TEL1* gene after stable transfection of TEL1rep in human A-T cells, RT-PCR analysis was performed. Using the *TEL1*-specific primers FOR3 and REV3, we were able to amplify 544 bp of the extreme 3′ end of the *TEL1* transcript in reverse-transcribed cDNA derived from pooled samples of TEL1rep-transfected cells but not from deltaTELrep-transfected or empty vector-transfected cells (Figure 1 B). Equal or 10-fold excess amounts of control RNA samples that have not been reverse transcribed gave no product in PCR analyses, thus ruling out the possibility of residual genomic or plasmid DNA in the RNA samples that might produce false-positive signals (data not shown). It has been shown previously that AT5BIVA cells contain no detectable *ATM*-RNA (Morgan *et al.*, 1997), thus ruling out false-positive RT-PCR products due to potential *ATM*-cDNA templates. In addition, the RT-PCR product was specific for the *TEL1*-RNA, since the primer combination and PCR conditions used did not amplify the homologous *ATM* sequences, as analyzed by RT-PCR in normal cells (data not shown). Based on our RT-PCR data, we thus conclude that the *TEL1* gene was transcribed in human A-T cells after stable transfection.

In four independent experiments, the growth characteristics of the transfected cell populations were determined based on Coulter counting. The deltaTELrep- and TEL1rep-transfected A-T cell lines were found to have slightly increased population doubling times (35.5 and 35.8 h, respectively) compared with their parent 5L13 (33.2 h). We conclude that differences in growth kinetics do not contribute to altered cellular phenotypes that were obtained after *TEL1* expression. Similarly, standard cytogenetic analyses of metaphase spreads revealed no differences in the karyotype between untreated transfected and parental populations (data not shown).

Table 1. Reduced spontaneous $lacZ^+$ conversion rates of *TEL1*-transfected A-T cells in fluctuation analyses

AT5BIVA cells (clone 5L13) transfected with	$lacZ^+$ cells detected	Cells screened	$lacZ^+$ conversion rate (events per 10^5 cells per generation)
Experiment 1			
pRep5	1136	6.1×10^6	3.9 (100%)
deltaTELrep	486	5.2×10^6	2.0 (51%)
TEL1rep	121	7.3×10^6	0.47 (12%)
Experiment 2			
pRep5	2105	1.0×10^6	35.7 (100%)
deltaTELrep	ND	ND	ND
TEL1rep	462	2.4×10^6	4.1 (11%)

A-T (AT5BIVA) cells harboring an integrated copy of the pLrec recombination vector (cell clone 5L13) were stably transfected with the TEL1rep, deltaTELrep, or empty pRep5 expression vectors and were tested for intrachromosomal recombination events that lead to reconstitution of the *lacZ* reporter gene as described in the MATERIALS AND METHODS section. ND, not determined.

TEL1 Expression Reduces Hyperrecombination in A-T Cells

Increased spontaneous recombination is one aspect of the intrinsic genomic instability observed in A-T cells (Meyn, 1993; Luo *et al.*, 1996). In order to measure the influence of *TEL1* expression on spontaneous intrachromosomal recombination rates in A-T cells, the rate of conversion to $lacZ^+$ cells was determined in two independent transfection and fluctuation experiments using the AT5BIVA derivative 5L13 that contains a chromosomally integrated pLrec recombination vector. Of 6.1×10^6 5L13 cells that were derived from a 5L13 subclone that was stably transfected with the empty vector pRep5, 1136 $lacZ^+$ cells were found that had undergone spontaneous intrachromosomal recombination (Table 1). In contrast, of 7.3×10^6 cells derived from a 5L13 subclone that was stably transfected with the TEL1rep expression construct, only 121 recombination events were detectable. The $lacZ^+$ conversion rate was thus reduced from 3.9×10^{-5} conversions per cell generation in pRep5-transfected control cells to 0.47×10^{-5} after TEL1rep transfection, which is 12% of the control rate. Interestingly, the conversion rate of deltaTELrep-transfected cells was also slightly reduced to 2.0×10^{-5}, which is 51% of the control level. In a second set of experiments involving different clonal isolates, the conversion rate of the pRep5-transfected clone was 35.7×10^{-5}. The rate in the TEL1rep-transfected subclone was again much lower than in the control: 4.1×10^{-5} conversions per cell generation or 11% of the control rate. The higher overall

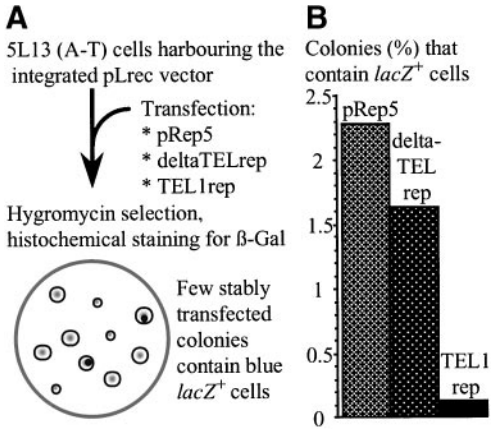

Figure 2. Reduced spontaneous conversion to $lacZ^+$-positive A-T cells after transfection with the *TEL1* expression vector. (A) Schematic depicting experimental procedure. (B) Colonies (%) that have been stably transfected with the *TEL1* expression vectors indicated and that contain $lacZ^+$ cells due to spontaneous recombination events within the pLrec recombination vector.

conversion rate in the second experiment most likely reflects changes in the recipient culture before transfection that altered chromatin structure or the copy number of the integrated pLrec recombination vector and, thus, promoted a higher basal rate of intrachromosomal recombination.

We also measured the frequency of 5L13 colonies that had been stably transformed to hyg^R and had undergone recombination of their *lacZ* genes following transfection with the *TEL1* expression vectors (Figure 2 A). The frequencies of hyg^R colonies that contained one or more $lacZ^+$ cells were 2.3% ($lacZ^+ = 63$; n = 2720) and 1.65% ($lacZ^+ = 31$; n = 1870) for A-T cells transfected with pRep5 and deltaTELrep, respectively (Figure 2B). In contrast, *TEL1* transfection in A-T cells resulted in a frequency of $LacZ^+$ colonies of 0.15% ($lacZ^+ = 1$; n = 672). Taken together, our different approaches to analyze intrachromosomal recombination rates in fluctuation experiments as well as in freshly transfected colonies show that expression of the yeast *TEL1* gene is able to suppress and thus partly complement the hyperrecombination phenotype of A-T fibroblasts.

TEL1rep Transfection Partly Complements Radiation Hypersensitivity of A-T Cells

A-T cells display, both in vitro and in vivo, an enhanced sensitivity to the cytotoxic effects of IR. To investigate the radioprotective effects of the Tel1 protein, we analyzed the radiosensitivity of stably *TEL1*-transfected A-T cells. In clonogenic colony survival assays (Figure 3 A), stably deltaTELrep-transfected A-T fibroblasts (GM5849) were not distinguishable from pRep5-transfected or untransfected parental cells and showed the typical hypersensitivity of A-T cells to the cytotoxic effects of IR (compare to GM0639). A-T cells transfected with the TEL1 construct (TEL1rep) showed a very mild but consistent resistance to IR as compared with their respective controls. Normal control fibroblasts GM0847 transfected with TEL1rep were not distinguishable from untransfected parental cells in clonogenic survival assays (data not shown).

We also measured IR-induced apotosis by fluorescence microscopy. After irradiation with 3 Gy, we observed the previously reported excess of apoptotic A-T cells (ATrep5) compared with normal cells (Meyn *et al.*, 1994; Fritz *et al.*, 1997; Uhrhammer *et al.*, 1999). In contrast, the pooled population of TEL1rep-transfected A-T cells clearly showed a reduction in their frequency of apoptotic cells throughout the 5 d analyzed (Figure 3B). In a separate experiment, A-T

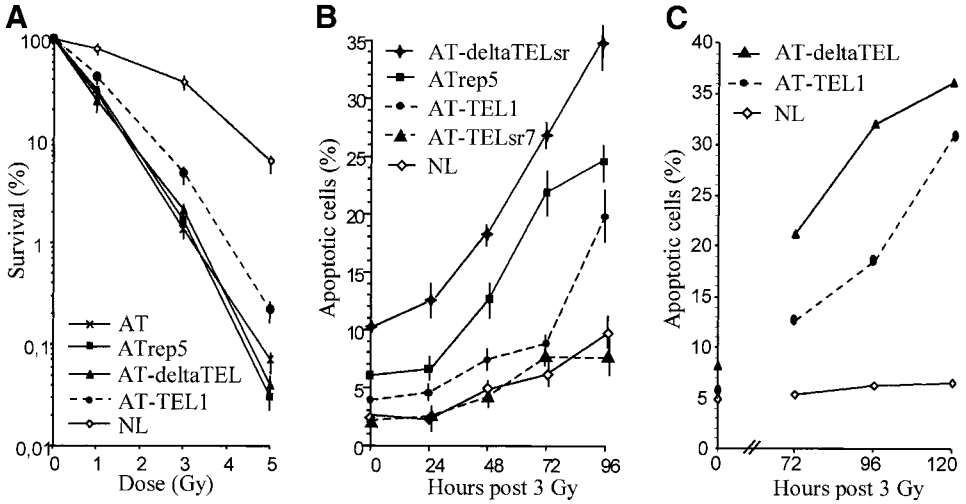

Figure 3. Reduced radiosensitivity of *TEL1*-transfected AT cells. Stably transfected A-T fibroblasts (GM5849) were analyzed for radiosensitivity in (A) clonogenic survival assays and (B) determination of apoptotic cells (%) after 3-Gy IR by fluorescence microscopy or (C) by FACS analysis. Designated populations are normal GM0639 (NL) cells or stably transfected A-T fibroblasts. AT, untransfected control AT cells; ATrep5, AT cells transfected with the empty expression vector pRep5; AT-deltaTEL, AT cells transfected with the truncated *TEL1* expression construct; AT-deltaTELsr, single clone derived from the pool of cells stably transfected with deltaTELrep after streptonigrin exposure; AT-TEL1, pool of TEL1rep-transfected A-T cells; AT-TELsr7, single clone derived from the pool of cells stably transfected with TEL1rep after streptonigrin exposure. (A) Mean values and SDs from three (AT, ATrep5, and AT-deltaTEL) or eight (AT-TEL1, NL) experiments, each plated in duplicates. (B) Mean values and SDs from three (ATrep5), five (AT-TELsr7), or seven (AT-deltaTELsr, AT-TEL1, NL) double-blind experiments; in each experiment at least 500 cells per point were scored. (C) Representative experiment showing FACS-based analysis of apoptotic subG1 cells after staining with propidium iodide.

cells were transfected with either TEL1rep or deltaTEL1rep and were exposed to the radiomimetic drug streptonigrin in a selection regimen, that allowed few nonresistant cells to survive. Individual clones that had grown after streptonigrin exposure then were tested for radiosensitivity. TEL1rep-transfected A-T subclones (e.g., AT-TELsr7) demonstrated even greater resistance to IR-induced apoptosis than the pooled population of TEL1rep transfectants (Figure 3B). In contrast, individual subclones of deltaTELrep-transfected A-T cells were even more radiosensitive than the empty vector-transfected A-T cell line, thus indicating that streptonigrin exposure per se did not lead to stable radiation resistant cells.

In an alternative assay, hypodiploid subG1 cells, indicative of cells that have undergone nuclear fragmentation during apoptosis, were determined by FACS analyses after staining with propidium iodide. In a representative experiment the fraction of hypodiploid cells in the deltaTELrep-transfected A-T population increased to 21%, 32%, and 36% within 3, 4, and 5 d, respectively, after 3-Gy IR. In contrast, TEL1rep-transfected A-T cells showed only 13%, 18%, and 31% of subG1 cells at the same time, again indicating the suppression of IR-induced apoptosis compared with the above controls (Figure 3C). Normal control fibroblasts GM0639 showed almost no induction of apoptosis in the same time range following 3-Gy irradiation. Taken together, we conclude from different experiments that *TEL1* expression suppresses the IR-induced apoptosis that occurs in A-T cells in the first 5 d after irradiation. In addition, *TEL1* expression leads to a mild radioprotection in colony survival assays when compared with the controls.

TEL1 Expression Extends the Length of Telomeres in A-T Cells

We measured the average lengths of telomeres in AT5BIVA fibroblasts and derivatives 4–16 mo after the transfection of *TEL1* expression vectors by analyzing independent genomic DNA isolates. In each of three experiments, the mean telomere sizes of transfected or control A-T populations were shorter than those of the normal control cell line GM0847 (Figure 4). However, we observed a clear increase in average telomere length in A-T cells that had been stably transformed with TEL1rep (Table 2). The mean telomere size was determined to be 2413 bp, and 2576 bp for independent DNA samples of untransfected A-T cells as well as 2617 bp, 2933 bp, and 3224 bp for a pool of deltaTEL-transfected A-T cells, which is in the same size range as that obtained earlier for the parental AT5BIVA cell line (Xia *et al.*, 1996; Smilenov *et al.*, 1997). In contrast, the mean telomere length in a pooled population of *TEL1*-transfected A-T cells was substantially increased, with TRF sizes of 4177 bp, 4230 bp, 4700 bp, 5078 bp, and 5283 bp in independent samples. Interestingly, the mean TRF size in the *TEL1*-transfected subclone TELsr7, which was obtained after streptonigrin exposure and proved to be highly resistant to IR-induced apoptosis, showed the highest mean TRF length (6194 bp).

In order to rule out the possibility that our TEL1rep-transfected, pooled population was inadvertently descendent from a (few) single clone(s) that overgrew the original pooled population of transfectants, we reisolated 20 random single clones from the pooled population and analyzed their telomere length. The individual subclones displayed extensive heterogeneity in their mean TRF lengths, suggesting that the pooled population was indeed derived from multiple transfectants and, thus, a representative sampling of the original transfectants (data not shown). Thus, we conclude, based on the TRF analyses, that the expression of the yeast *TEL1* gene increased the length of telomeric repeat tracts in A-T cells.

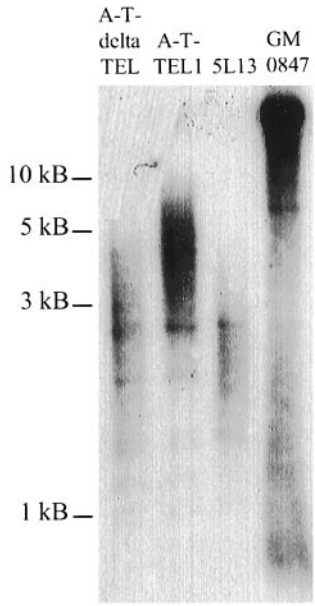

Figure 4. Analysis of TRF length in normal control cells (GM0847) and A-T (5L13) cells transfected with *TEL1* expression vectors. Genomic DNA from cells was isolated, digested with *Alu*I over night, separated on 0.8% agarose gels, blotted on nylon membranes, and hybridized to P^{32}-labeled high molecular telomeric probes. Following autoradiography, telomeric restriction fragments were detected. After scanning the films, the mean TRF length was determined as the peak intensity of the TRF signals and the size calculated after comparing the size standards. The mean TRF length was determined to be 2413 bp, 2617 bp, and 4177 bp, respectively, for 5L13, ATdeltaTEL, and AT-TEL1 cells, while the normal cell line GM0847 had substantially longer telomeres above 10 kB.

Table 2. Increased mean TRF length in stably *TEL1*-transfected A-T cells

Cell line	Mean TRF length (bp)
5L13	2413, 2567
ATdeltaTEL	2617, 2933, 3224
AT-TEL1	4177, 4230, 4700, 5078, 5283, 6194 (sr7)

Parental 5L13 (A-T) cells were stably transfected with the TEL1rep (AT-TEL1) or deltaTELrep (ATdeltaTEL) expression vectors, and genomic DNA was analyzed for the TRF length representing the length of telomeric repeat tracts, as described in the Materials and Methods section. Each number represents the mean TRF length (bp) found in independent DNA samples of the respective cell line.

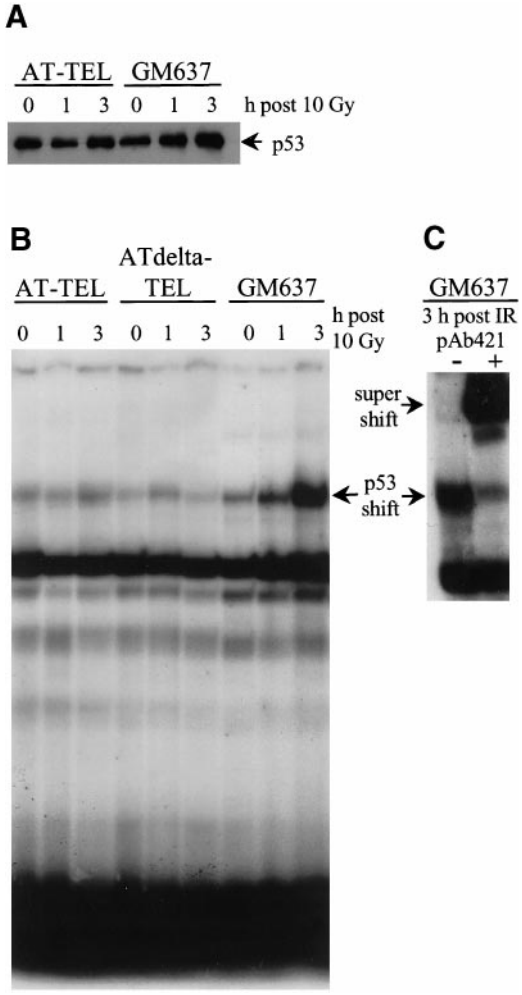

Figure 5. The expression of *TEL1* has no effect on basic p53 protein levels and IR-induced p53 accumulation in A-T cells. Nuclear extracts were prepared following 10-Gy IR and p53 protein was detected in Western analyses (A). Normal GM637 cells showed a time-dependent p53 accumulation upon IR, while *TEL1*-transfected A-T cells failed to accumulate p53. This typical A-T deficiency also was confirmed in A-T control cells (not shown). (B) p53 protein was shifted with oligonucleotides containing the p53 consensus sequence from *GADD45*, again showing the clear accumulation of active, DNA-binding p53 protein upon IR in normal GM637 cells. Neither A-T cell line showed an accumulation of DNA-bound p53 upon IR. Supershift analyses using anti-p53 antibody pAb421 confirmed the specificity of the shifted p53 bands (C).

TEL1 Expression Has No Effect on Basic p53 Protein Levels and IR-Induced p53 Stabilization

IR-induced p53 accumulation has been shown to be reduced and delayed in cells from A-T patients (Kastan *et al.*, 1992). Various lines of evidence suggest that the C-terminal PI3-kinase domain of ATM may directly phosphorylate and thus stabilize p53 in response to IR. In order to investigate whether the highly homologous phosphatidyl-inositol-3-kinase (PI3K) domain of Tel1p may exert similar functions in A-T cells, which then may contribute to the complementation of cellular phenotypes, we analyzed p53 stabilization in *TEL1*-transfected cells. Nuclear extracts from *TEL1*-transfected A-T cells and normal GM637 cells were prepared 1 and 3 h after irradiation (10 Gy), and p53 protein was quantitated in Western analyses. As shown in Figure 5A, normal GM637 control cells clearly accumulated p53 protein following IR, while the *TEL1*-transfected A-T cells showed no accumulation. *TEL1*-transfected A-T cells thus showed the typical A-T deficiency, which also was confirmed in deltaTEL-transfected and untransfected A-T cells (data not shown).

It has been described that basic p53 protein levels are high in SV40-transformed cells, which may diminish the detection of IR-induced accumulation of transcriptionally active p53 (Kohli and Jorgensen, 1999). We therefore performed electrophoretic mobility shift analyses with nuclear extracts in order to detect IR-induced stabilization of active, DNA-binding p53 rather than analyzing the bulk p53 protein amount in Western analyses. Nuclear extracts were incubated with radioactively labeled oligonucleotides carrying a p53 consensus-binding sequence from the GADD45 promotor. Electrophoretic mobility shift experiments (Figure 5B) showed an unspecific band as well as the shifted p53 protein bound to the consensus DNA sequence. In control experiments, the specificity of the p53 band was confirmed after preincubation with anti-p53 antibody (pAb421) leading to a supershifted band arising from a trimeric complex consisting of p53 protein, anti-p53 antibody, and the bound oligonucleotides (Figure 5C). In the shifted p53 bands, a clear time-dependent accumulation of active p53 protein was observed in control GM637 fibroblasts following IR. In contrast, the control A-T cell line (A-TdeltaTEL) showed no accumulation of oligonucleotide-bound p53 following 10 Gy of IR, thus again illustrating the typical A-T deficiency. The same lack of IR-induced p53 accumulation also is evident in the *TEL1*-transfected A-T population, indicating that the Tel1 protein did not complement this deficiency. Taken together, we conclude from Western analyses and EMSAs that constitutive *TEL1* expression in A-T cells has no effect on basic p53 amounts and IR-induced p53 accumulation.

DISCUSSION

In the present work, we report that specific aspects of the A-T cellular phenotype, i.e., hyperrecombination, hypersensitivity to IR-induced apoptosis, and telomere shortening, are partially suppressed upon the stable introduction of an expression vector containing the *S. cerevisiae TEL1* gene.

Expression of the Yeast TEL1 Gene in Human A-T Cells Is Linked to Phenotypic Complementation

Transcription of the TEL1rep expression construct leads to the production of an RNA of ~9500 bp encoding the 3′ end of yeast ribosomal protein L17a as well as the complete *TEL1* gene. Using RT-PCR, we identified the presence of the extreme 3′ end of the *TEL1* RNA in TEL1rep-transfected A-T cells, but not in control deltaTELrep-transfected cells. We thus conclude that the yeast *TEL1* gene is transcribed in the *TEL1*-transfected cells. Confirmation of Tel1p protein expression was attempted through the use of Western blotting and immunofluorescence. However, the two anti-Tel1p an-

tibodies available to us lacked the specificity needed to conclusively demonstrate Tel1p expression (data not shown). In control experiments, high protein expression from stably transfected genes in A-T cells using the pRep5 vector was confirmed by using a reporter gene encoding green fluorescent protein (data not shown).

TEL1 Expression Has No Effect on Basic and IR-Induced p53 Stabilization

ATM binds to p53 in vivo (Watters *et al.*, 1997) and phosphorylates p53 on Ser^{15} in vitro (Banin *et al.*, 1998; Canman *et al.*, 1998), thus strongly suggesting that ATM is a protein kinase that phosphorylates and stabilizes p53 in vivo upon IR. Since Tel1p shares 45% amino acid identity in the kinase domain with ATM, and since *TEL1* controls damage-induced phosphorylation of Rfa2p, Rad53p, and Rad9p in yeast (Brush *et al.*, 1996; Sugimoto *et al.*, 1997; Emili, 1998; Vialard *et al.*, 1998), we asked whether Tel1p may modulate p53 in transfected A-T cells and, thus, contribute to the complementation of cellular phenotypes. Although p53 is bound and, thus, inactivated by a large T-antigen in SV40-transformed cells, a retained regulatory mechanism of p53 activity in SV40-transformed human cells has been suggested (Jung *et al.*, 1997). Indeed, both our Western analyses and electrophoretic mobility shift analyses clearly show that SV40-immortalized GM637 cells are capable of accumulating p53 upon IR, which is in agreement with recent data obtained by analyzing p53-dependent p21 protein induction following IR (Kohli and Jorgensen, 1999). Although SV40-immortalized, the A-T fibroblasts used in our studies also showed detectable amounts of active p53 in the oligonucleotide-shifted band. Upon constitutive *TEL1* expression, however, we found neither differences in basic p53 protein levels nor increased amounts of p53 protein following IR. The latter may represent the typical A-T deficiency or may be due to blunted p53 response following IR by the SV40 influence in this particular cell line. In any case, we can conclude that the expression of *TEL1* in A-T cells had no effect on basic or IR-induced p53 stabilization, and we thus propose that the complementation of cellular phenotypes obtained after *TEL1* expression is independent of biochemical p53 activation.

TEL1 Expression in A-T Cells Suppresses Spontaneous Intrachromosomal Hyperrecombination

TEL1-deficient yeast strains and A-T cells both express genomic instability, as manifested by increased mitotic recombination and chromosome loss. Interchromosomal recombination in *TEL1* yeast mutants and in A-T cells are elevated ~4-fold and 10-fold, respectively, compared with their wild-type controls (Greenwell *et al.*, 1995; Luo *et al.*, 1996). In addition, intrachromosomal recombination has been shown to be increased 30–200-fold in A-T cells (Meyn, 1993; Luo *et al.*, 1996). By using the the pLrec recombination vector in fluctuation analyses and colony conversion experiments, we found that the expression of the full-length yeast *TEL1* gene is associated with the suppression of the spontaneous intrachromosomal recombination rate to ~10% of that observed in the parental A-T cell line. Whether the twofold reduction of recombination rates observed upon transfection of the deltaTELrep expression construct is significant and is due to the expression of a highly truncated but partially active Tel1 protein remains to be determined.

The etiology of the A-T hyperrecombination phenotype is not known. We initially proposed that hyperrecombination and other forms of genetic instability seen in A-T cells arise indirectly from defects in cell cycle checkpoints (Meyn, 1993), an explanation that was supported by the subsequent demonstration that the loss of p53-mediated cell cycle checkpoints is associated with increased spontaneous recombination in mammalian cells (Meyn *et al.*, 1994). However, we do not find any evidence for the restoration of radiation-induced cell cycle checkpoints in A-T cells stably transfected with *TEL1*, as measured by bivariate FACS analyses (data not shown). The ability of Tel1p to suppress hyperrecombination in A-T fibroblasts without correcting their cell cycle checkpoint and p53 stabilization defects suggests that the hyperrecombination phenotype of A-T cells is not primarily due to a lack of cell cycle checkpoints or to an inability to trigger p53-mediated cellular responses through ATM signaling.

TEL1 Partially Complements A-T Radiosensitivity

Although *tel1*-deficient yeast strains are not hypersensitive to IR, an extra copy of *TEL1* in a *mec1*-deficient background has been shown to complement *mec1* radiosensitivity, suggesting that Tel1p and Mec1p act synergistically to provide radioresistance in yeast (Morrow *et al.*, 1995; Sanchez *et al.*, 1996). We now find that, as with *mec1* yeast mutants, *TEL1* expression can help protect *ATM*-deficient human cells from the cytotoxic effects of IR. Given the fact that even expression of wild-type hATM does not necessarily fully complement radiosensitivity of A-T cells (Zhang *et al.*, 1997), only a moderate complementation of IR hypersensitivity by the yeast *TEL1* gene may be expected. Indeed, colony survival after IR is only slightly improved by *TEL1* expression. However, we see in the pooled population of TEL1rep-transfected cells a clear time-dependent inhibition of the excessive IR-induced apoptosis typically found in AT5BIVA fibroblasts. Complementation of IR-induced apoptosis is even stronger in some individual TEL1rep subclones that had been isolated following exposure to streptonigrin (e.g., clone TELsr7). This is in marked contrast to the corresponding deltaTELrep-transfected subclones, which never showed increased resistance to IR. This effect may be due to higher than usual expression levels of the *TEL1* gene in these subclones of the pooled TEL1rep-transfected population, a hypothesis that is supported by the observation that one of these radioresistant subclones, TELsr7, has longer telomeres than a pooled population of TEL1rep-transfected A-T cells.

Why does the striking decrease in the apoptotic fraction of irradiated A-T cells not translate into a much better colony survival after IR? *TEL1* expression may not cause a large-scale reduction in the total number of A-T cells that undergo apoptosis. Instead, its primary effect may be to delay the onset of apoptosis beyond the usual 5 d in which apoptosis peaks both in A-T and normal human fibroblasts. In this regard, Takagi *et al.* (1998) have shown recently that lymphoblastoid cells derived from A-T donors are resistant to the early onset of IR-induced apoptosis but are unusually sensitive to the late onset of apoptosis 6 d postirradiation. This suggests the existence of temporally different mechanisms of apoptosis induction that may contribute to cellular

radiosensitivity. Alternatively, apoptosis may be efficiently blocked by the expression of the *TEL1* gene, but IR-induced cell death then may occur through other, as yet undefined, mechanisms that are not complemented. As pointed out by others, the mechanism of death in irradiated A-T cells is not fully understood but may include apoptosis, inefficient or error-prone repair of DNA double-strand breaks, or chromosome breaks (reviewed in Foray *et al.*, 1997; Dikomey *et al.*, 1998; Sikpi *et al.*, 1998), deficiency in cell cycle control (Beamish and Lavin, 1994), and structural alterations in the cytoskeleton (Mirzayans *et al.*, 1989).

TEL1 Expression Leads to Telomere Lengthening in A-T Cells

Primary A-T fibroblasts and lymphocytes as well as transformed A-T fibroblasts and lymphoblasts have been found to have unusually short telomeres (Kojis *et al.*, 1991; Pandita *et al.*, 1995; Metcalfe *et al.*, 1996; Xia *et al.*, 1996; for a dissecting report see Sprung *et al.*, 1997). Additional support for a functional role of ATM in controlling telomere length is provided by the demonstration that expression of a dominant-negative ATM fragment in normal cells results in a decrease in average telomere repeat length (Smilenov *et al.*, 1997). In yeast, deficiency of the homologous *TEL1* gene also leads to gradual telomere shortening (Lustig and Petes, 1986; Greenwell *et al.*, 1995; Ritchie *et al.*, 1999).

While the length of telomeres decreases with each cell division in primary cells, the average telomere length of immortalized, telomerase-positive cells is generally stable during long-term culture (Counter *et al.*, 1992; Counter *et al.*, 1994; Klingelhutz *et al.*, 1994; Bryan *et al.*, 1998). Consistent with these observations, the mean TRF length in our AT5BIVA cell line did not obviously change within 12 mo of continuous cultivating and was very similar to the TRF lengths reported for the same cell line by other researchers (Xia *et al.*, 1996; Smilenov *et al.*, 1997). From this we conclude that the telomere length in AT5BIVA is stable at least over the period of our experiments. However, after 4 mo of continuous culturing following transfection, the mean telomere lengths of *TEL1*-transfected AT5BIVA cells increased to almost double those of the parental A-T line (Figure 4). This was not the case in the deltaTEL-transfected control AT5BIVA population, which has the same population doubling time as *TEL1*-transfected cells. Since our analysis of TRF length is based on examining pooled populations of stably transfected cells, our results are not due to having chosen an individual TEL1rep-transfectant with unusually long telomeres. Thus, we conclude that the expression of the *TEL1* gene is causing telomere lengthening in A-T cells, independent of experimental procedures or variations in population doubling times.

Cellular control of telomere length is complex, and the precise roles that Tel1p and ATM play in telomere metabolism are uncertain. However, some initial insights are possible. The short telomeres seen in A-T cells and the complementation of this phenotype by *TEL1* expression are unlikely to be due to changes in telomerase activity. The short telomere phenotype is found in both A-T cells that express strong telomerase activity (e.g., the SV40-transformed fibroblasts used for our experiments) and in A-T cells that lack telomerase activity (primary diploid fibroblasts and lymphocytes) (e.g., Xia *et al.*, 1996). This conclusion is further supported by recent findings in *S. cerevisiae* that indicate that the role of Tel1p in telomere length control is at least partially independent of telomerase function (Ritchie *et al.*, 1999). The telomere lengthening seen in *TEL1*-transfected A-T cells is also unlikely to be the result of activating the so-called ALT pathway, in that our stably *TEL1*-transfected A-T cells did not show the extensive heterogeneity and bimodal distribution of telomere length that is characteristic for this mechanism of telomere extension (Murnane *et al.*, 1994; Bryan *et al.*, 1995; Sprung *et al.*, 1997).

We previously proposed that ATM normally monitors telomere length and initiates cell cycle arrest when telomeres shrink below a critical length (Meyn, 1995). However, we now find that the telomeres of A-T cells lengthen following transfection with the *TEL1* gene even though *TEL1* transfection does not correct the cell cycle checkpoint defects of these cells. This observation suggests that the short telomere phenotype of A-T cells is not caused by cell cycle checkpoint defects and is consistent with the recent demonstration that the effect of the ATM-homologue rad3p on telomere length in *Schizosaccharomyces pombe* is independent of the downstream cell cycle checkpoint proteins chk1 and cds1 (Matsuura *et al.*, 1999). In addition, the effect of *TEL1* expression on telomere length does not appear to be dependent on activating p53-mediated ATM signaling pathways. *TEL1* expression complements both the short telomere and the hyperrecombination phenotypes of transformed A-T fibroblasts, raising the possibility that both of these two phenotypes are caused by increased mitotic recombination. In this scenario, telomeric repeat tracts are more likely to undergo recombinational events that reduce their length in A-T cells than is the case in normal cells. The suppression of recombinational telomere loss through *TEL1* expression would then lead to a net increase of telomere length through telomerase-mediated elongation. In yeast, however, telomere rapid deletion, a form of telomere length reduction that quickly reduces the length of individual telomeres and that is thought to be mediated by intrachromatid recombination (Li and Lustig, 1996), is not affected by *tel1* mutation. Instead, the loss of telomere repeats upon *TEL1* inactivation is a slow process that requires at least 100 cell divisions to reach maximal telomere length reduction (Lustig and Petes, 1986; Runge and Zakian, 1996). These observations provide direct evidence against the idea that telomere shortening in *tel1*-deficient yeast cells is due to cellular hyperrecombination. Our demonstration that *TEL1* expression complements the short telomere phenotype of A-T cells allows the extension of this argument to the human situation and leads to the conclusion that it is unlikely that the short telomere phenotype in A-T cells is the result of deletional recombination of telomeric repeats.

TEL1 expression partially reverses radiosensitivity, hyperrecombination, and telomere shortening in A-T cells but does not correct their defects in cell cycle checkpoints and p53 induction. These results suggest that functions that determine the latter two phenotypes in human cells may reside in ATM domains that require a higher degree of homology than is present in the yeast Tel1 protein, or, alternatively, may reside in other functional yeast homologues. In this regard, it has been shown that Mec1p in *S. cerevisiae* and Rad3p in *S. pombe,* which are yeast homologues of ATM and putative partners of Tel1p, are involved in cell cycle regula-

tion and radiosensitivity, thus sharing functional properties with ATM that are different from those of Tel1p (Jimenez *et al.*, 1992; Bentley *et al.*, 1996; Siede *et al.*, 1996; Sun *et al.*, 1996; Gatti, 1998).

In the course of our experiments, the phenotypic characterization of the ATM protein has been examined by expressing different parts of *ATM* as well as the complete *ATM* cDNA (Morgan *et al.*, 1997; Zhang *et al.*, 1997; Ziv *et al.*, 1997) in A-T cells. Overexpression of the PI3 kinase domain alone was described to partially complement radioresistant DNA synthesis, radiosensitivity, and the frequency of IR-induced chromosome breaks (Morgan *et al.*, 1997). However, experiments indicating whether the expression of the PI3-K domain or the expression of full-length ATM (Zhang *et al.*, 1997; Ziv *et al.*, 1997) leads to increases in telomere length and/or suppression of hyperrecombination have not been reported. Through the complementation of a specific subset of defective A-T-phenotypes, *TEL1*-transfected A-T cells may provide useful tools to uncouple and decipher the different cellular pathways regulated by ATM. Further analyses of protein expression and activity in *TEL1*-complemented A-T cells may result in the linkage of specific ATM-regulated proteins and signaling pathways with specific cellular and clinical abnormalities. Based on the high structural conservation between the ATM and Tel1p proteins, cross-complementation of human A-T cells with the yeast *TEL1* gene has proven successful in functionally complementing specific cellular phenotypes. Given the powerful genetic tools in yeast, the reciprocal experiment of cross-complementing yeast mutants that are defective in *ATM* homologues or specific DNA repair-related genes with the human *ATM* gene also may provide valuable information on ATM functions.

ACKNOWLEDGMENTS

The authors thank T. Petes for the pSP21 and pPG40 plasmids harboring the yeast *TEL1* gene, R. Carbone for FACS analyses, and U. Hamm for technical assistance. This work was supported by the A-T Children's Project (E.F. and M.S.M.), the A-T Medical Research Foundation (M.S.M.), the National Institutes of Health grant R01 CA60592 (E.F. and M.S.M.) and the European Community grant F14PCT950010 (E.F., F.E.-S.).

REFERENCES

Aurias, A., Dutrillaux, B., Buriot, D., and Lejeune, J. (1980). High frequencies of inversions and translocations of chromosomes 7 and 14 in ataxia telangiectasia. Mutat. Res. *69*, 369–74.

Banin, S., Moyal, L., Shieh, S., Taya, Y., Anderson, C.W., Chessa, L., Smorodinsky, N.I., Prives, C., Reiss, Y., Shiloh, Y., and Ziv, Y. (1998). Enhanced phosphorylation of p53 by ATM in response to DNA damage. Science *281*, 1674–1677.

Baskaran, R., Wood, L.D., Whitaker, L.L., Canman, C.E., Morgan, S.E., Xu, Y., Barlow, C., Baltimore, D., Wynshaw-Boris, A., Kastan, M.B., and Wang, J.Y. (1997). Ataxia telangiectasia mutant protein activates c-Abl tyrosine kinase in response to ionizing radiation. Nature *387*, 516–519.

Beamish, H., and Lavin, M.F. (1994). Radiosensitivity in ataxia-telangiectasia: anomalies in radiation-induced cell cycle delay. Int. J. Radiat. Biol. *65*, 175–184.

Bentley, N.J., Holtzman, D.A., Flaggs, G., Keegan, K.S., DeMaggio, A., Ford, J.C., Hoekstra, M., and Carr, A.M. The Schizosaccharomyces pombe rad3 checkpoint gene. EMBO J. *15*, 6641–6651

Brush, G.S., Morrow, D.M., Hieter, P., and Kelly, T.J. (1996). The ATM homologue MEC1 is required for phosphorylation of replication protein A in yeast. Proc. Natl. Acad. Sci. USA *93*, 15075–15080.

Bryan, T.M., Englezou, A., Dunham, M.A., and Reddel, R.R. (1998). Telomere length dynamics in telomerase-positive immortal human cell populations. Exp. Cell Res. *239*, 370–378.

Bryan, T.M., Englezou, A., Gupta, J., Bacchetti, S., and Reddel, R.R. (1995). Telomere elongation in immortal human cells without detectable telomerase activity. EMBO J. *14*, 4240–4248.

Canman, C.E., Lim, D.S., Cimprich, K.A., Taya, Y., Tamai, K., Sakaguchi, K., Appella, E., Kastan, M.B., and Siliciano, J.D. (1998). Activation of the ATM kinase by ionizing radiation and phosphorylation of p53. Science *281*, 1677–1679.

Capizzi, R.L., and Jameson, J.W. (1972). A table for the estimation of the spontaneous mutation rate of cells in culture. Mutat. Res. *17*, 147–148.

Carney, J.P. (1999). Chromosomal breakage syndromes. Curr. Opin. Immunol. *11*, 443–447.

Chen, Z., Fadiel, A., Jia, J.F., Sakamoto, H., Carbone, R., and Naftolin, F. (1999). Induction of apoptosis and suppression of clonogenicity of ovarian carcinoma cells with estrogen mustard. Cancer *85*, 2616–2622.

Counter, C.M., Avilion, A.A., LeFeuvre, C.E., Stewart, N.G., Greider, C.W., Harley, C.B., and Bacchetti, S. (1992). Telomere shortening associated with chromosome instability is arrested in immortal cells which express telomerase activity. EMBO J. *11*, 1921–1929.

Counter, C.M., Bothelo, F.M., Wang, P., Harley, C.B., and Bacchetti, S. (1994). Stabilization of short telomeres and telomerase activity accompany immortalization of Epstein-Barr virus-transformed human B lymphozytes. J. Virol. *68*, 3410–3414.

Dikomey, E., Dahm-Daphi, J., Brammer, I., Martensen, R., and Kaina, B. (1998). Correlation between cellular radiosensitivity and non-repaired double-strand breaks studied in nine mammalian cell lines. Int. J. Radiat. Biol. *73*, 269–278.

Duchaud, E., Ridet, A., Stoppa-Lyonnet, D., Janin, N., Moustacchi, E., and Rosselli, F. (1996). Deregulated apoptosis in ataxia telangiectasia: association with clinical stigmata and radiosensitivity. Cancer Res. *56*, 1400–1404.

Emili, A. (1998). MEC1-dependent phosphorylation of Rad9p in response to DNA damage. Mol. Cell *2*, 183–189.

Foray, N., Badie, C., Arlett, C.F., and Malaise, E.P. (1997). Comments on the paper: the ATM gene and the radiobiology of ataxia-telangiectasia. Int. J. Radiat. Biol. *71*, 449–450.

Fritz, E., Elsea, S.H., Patel, P.I., and Meyn, M.S. (1997). Overexpression of a truncated human topoisomerase III partially corrects multiple aspects of the ataxia-telangiectasia phenotype. Proc. Natl. Acad. Sci. USA *94*, 4538–4542.

Gatti, R.A., Berkel, I., Boder, E., Braedt, G., Charmley, P., Concannon, P., Ersoy, F., Foroud, T., Jaspers, N.G., Lange, K., Lathrop, K.M., Leppert, M., Nakamura, Y., O'Conner, P., Paterson, M., Salser, W., Sanal, O., Silver, J., Sparkes, R.S., Susi, E., Weeks, D.E., Wei, S., White, R., and Yoder, F. (1988). Localization of an ataxia-telangiectasia gene to chromosome 11q22-23. Nature *336*, 577–580.

Gatti, R.A. (1998). In: Ataxia-telangiectasia, eds. B. Vogelstein, and K.W. Kinzler, New York, NY: McGraw-Hill, pp. 275–300.

Gilad, S., Khosravi, R., Shkedy, D., Uziel, T., Ziv, Y., Savitsky, K., Rotman, G., Smith, S., Cheesa, L., Jorgensen, T.J., Hanik, R., Frydman, M., Sanal, O., Portnoi, S., Goldwicz, Z., Jaspers, N.G.J., Gatti, R.A., Lenoid, G., Lavin, M.F., Tatsumi, K., Wegner, R.D., Shiloh, Y.,

and Bar-Shira, A. (1996). Predominance of null mutations in ataxia-telangiectasia. Hum. Mol. Genet. *5*, 433–439.

Greenwell, P.W., Kronmal, S.L., Porter, S.E., Gassenhuber, J., Obermaier, B., and Petes, T.D. (1995). *TEL1*, a gene involved in controlling telomere length in *S. cerevisiae*, is homologous to the human ataxia telangiectasia gene. Cell *82*, 823–829.

Groger, R.K., Morrow, D.M., and Tykocinski, M.L. (1989). Directional antisense and sense cDNA cloning using Epstein-Barr virus episomal expression vectors [published erratum appears in Gene 1989 83(2):395]. Gene *81*, 285–294.

Hoekstra, M.F. (1997). Responses to DNA. damage and regulation of cell cycle checkpoints by the ATM protein kinase family. Curr. Opin. Genet. Dev. *7*, 170–175.

Ijdo, J.W., Wells, R.A., Baldini, A., and Reeders, S.T. (1991). Improved telomere detection using a telomere repeat probe (TTAGGG)n generated by PCR. Nucleic Acids Res. *19*, 4780.

Jimenez, G., Yucel, J., Rowley, R., and Subramani, S. (1992). The rad3+ gene of Schizosaccharomyces pombe is involved in multiple checkpoint functions and in DNA repair. Proc. Natl. Acad. Sci. USA *89*, 4952–4956.

Jung, M., Lee, S.A., Zhang, Y., and Dritschilo, A. (1997). Regulation of p53 in response to ionizing radiation in ataxia telangiectasia fibroblasts. Int. J. Radiat. Oncol. Biol. Phys. *37*, 417–422.

Kastan, M.B., Zhan, Q., el-Deiry, W.S., Carrier, F., Jacks, T., Walsh, W.V., Plunkett, B.S., Vogelstein, B., and Fornace, A.J.J. (1992). A mammalian cell cycle checkpoint pathway utilizing p53 and GADD45 is defective in ataxia-telangiectasia. Cell *71*, 587–597.

Keegan, K.S., Holtzman, D.A., Plug, A.W., Christenson, E.R., Brainerd, E.E., Flaggs, G., Bentley, N.J., Taylor, E.M., Meyn, M.S., Moss, S.B., Carr, A.M., Ashley, T., and Hoekstra, M.F. (1996). The Atr and Atm protein kinases associate with different sites along meiotically pairing chromosomes. Genes Dev. *10*, 2423–2437.

Keith, C.T., and Schreiber, S.L. (1995). PIK-related kinases: DNA repair, recombination, and cell cycle checkpoints. Science *270*, 50–51.

Kharbanda, S., Yuan, Z.M., Weichselbaum, R., and Kufe, D. (1998). Determination of cell fate by c-Abl activation in the response to DNA damage. Oncogene *17*, 3309–3318.

Klingelhutz, A.J., Barber, S.A., Smith, P.P., Dyer, K., and McDougall, J.K. (1994). Restoration of telomeres in human papillomavirus-transformed human anogenital epithelial cells. Mol. Cell. Biol. *14*, 961–969.

Kohli, M., and Jorgensen, T.J. (1999). The influence of SV40 immortalization of human fibroblasts on p53-dependent radiation responses. Biochem. Biophys. Res. Commun. *257*, 168–176.

Kojis, T.L., Gatti, R.A., and Sparkes, R.S. (1991). The cytogenetics of ataxia telangiectasia. Cancer Genet. Cytogenet. *56*, 143–156.

Lakin, N.D., Weber, P., Stankovic, T., Rottinghaus, S.T., Taylor, A.M., and Jackson, S.P. (1996). Analysis of the ATM protein in wild-type and ataxia telangiectasia cells. Oncogene *13*, 2707–2716.

Lavin, M.F., and Shiloh, Y. (1997). The genetic defect in ataxia-telangiectasis. Annu. Rev. Genet. *15*, 177–202.

Leer, R.J., van Raamsdonk-Duin, M.M., Hagendoorn, M.J., Mager, W.H., and Planta, R.J. (1984). Structural comparison of yeast ribosomal protein genes. Nucleic Acids. Res. *12*, 6685–6700.

Li, B., and Lustig, A.J. (1996). A novel mechanism for telomere size control in *Saccharomyces cerevisiae*. Genes Dev. *10*, 1310–1326.

Luo, C.M., Tang, W., Mekeel, K.L., DeFrank, J.S., Anné, P.R., and Powell, S.N. (1996). High frequency and error-prone DNA recombination in ataxia telangiectasia cell lines. J. Biol. Chem. *271*, 4497–4503.

Lustig, A.J., and Petes, T.D. (1986). Identification of yeast mutants with altered telomere structure. Proc. Natl. Acad. Sci. USA *83*, 1398–1402.

Matsuura, A., Naito, T., and Ishikawa, F. (1999). Genetic control of telomere integrity in Schizosaccharomyces pombe: rad3(+) and tel1(+) are parts of two regulatory networks independent of the downstream protein kinases chk1(+) and cds1(+). Genetics *152*, 1501–1512.

Metcalfe, J.A., Parkhill, J., Campbell, L., Stacey, M., Biggs, P., Byrd, P.J., and Taylor, A.M. (1996). Accelerated telomere shortening in ataxia telangiectasia. Nat. Genet. *13*, 350–353.

Meyn, M.S. (1995). Ataxia-telangiectasia and cellular responses to DNA damage. Cancer Res. *55*, 5991–6001.

Meyn, M.S. (1993). High spontaneous intrachromosomal recombination rates in ataxia-telangiectasia. Science *260*, 1327–1330.

Meyn, M.S., Lu-Kuo, J.M., and Herzing, L.B. (1993). Expression cloning of multiple human cDNAs that complement the phenotypic defects of ataxia-telangiectasia group D fibroblasts. Am. J. Hum. Genet. *53*, 1206–1216.

Meyn, M.S., Strasfeld, L., and Allen, C. (1994). Testing the role of p53 in the expression of genetic instability and apoptosis in ataxia-telangiectasia. Int. J. Radiat. Biol. *66*, S141–S149.

Meyn, M.S. (1999). Ataxia-telangiectasia, cancer and the pathobiology of the ATM gene. Clin Genet. *55*, 289–304.

Mirzayans, R., Smith, B.P., and Paterson, M.C. (1989). Hypersensitivity to cell killing and faulty repair of 1-beta-D-arabinofuranosylcytosine-detectable sites in human (ataxia-telangiectasia) fibroblasts treated with 4-nitroquinoline 1-oxide. Cancer Res. *49*, 5523–5529.

Morgan, S.E., Lovly, C., Pandita, T.K., Shiloh, Y., and Kastan, M.B. (1997). Fragments of ATM which have dominant-negative or complementing activity. Mol. Cell. Biol. *17*, 2020–2029.

Morrow, D.M., Tagle, D.A., Shiloh, Y., Collins, F.S., and Hieter, P. (1995). *TEL1*, an *S. cerevisiae* homolog of the human gene mutated in ataxia telangiectasia, is functionally related to the yeast checkpoint gene *MEC1*. Cell *82*, 831–840.

Murnane, J.P., Sabatier, L., Marder, B.A., and Morgan, W.F. (1994). Telomere dynamics in an immortal human cell line. EMBO J. *13*, 4953–4962.

Oexle, K. (1998). Telomere length distribution and Southern blot analysis. J. Theor. Biol. *190*, 369–377.

Pandita, T.K., Pathak, S., and Geard, C.R. (1995). Chromosome end associations, telomeres and telomerase activity in ataxia telangiectasia cells. Cytogenet. Cell. Genet. *71*, 86–93.

Ritchie, K.B., Mallory, J.C., and Petes, T.D. (1999). Interactions of *TLC1* (which encodes the RNA subunit of telomerase), *TEL1*, and *MEC1* in regulating telomere length in the yeast *Saccharomyces cerevisiae*. Mol. Cell. Biol. *19*, 6065–6075.

Rotman, G., and Shiloh, Y. (1998). ATM: from gene to function. Hum. Mol. Genet. *7*, 1555–1563.

Runge, K.W., and Zakian, V.A. (1996). TEL2, an essential gene required for telomere length regulation and telomere position effect in *Saccharomyces cerevisiae*. Mol. Cell. Biol. *16*, 3094–3105.

Sanchez, Y., Desany, B.A., Jones, W.J., Liu, Q., Wang, B., and Elledge, S.J. (1996). Regulation of RAD53 by the ATM-like kinases *MEC1* and *TEL1* in yeast cell cycle checkpoint pathways. Science *271*, 357–360.

Savitsky, K., Bar-Shira, A., Gilad, S., Rotman, G., Ziv, Y., Vanagaite, L., Tagle, D.A., Smith, S., Uziel, T., Sfez, S., Ashkenazi, M., Pecker, I., Frydman, M., Harnik, R., Patanjali, S.R., Simmons, A., Clines, G.A., Sartiel, A., Gatti, R.A., Chessa, L., Sanal, O., Lavin, M.F., Jaspers, N.G.J., Taylor, M.R., Arlett, C.A., Miki, T., Weissman, S.M.,

Lovett, M., Collins, F.S., and Shiloh, Y. (1995a). A single ataxia telangiectasia gene with a product similar to PI-3 kinase. Science. *268*, 1749–1753.

Savitsky, K., Sfez, S., Tagle, D.A., Ziv, Y., Sartiel, A., Collins, F.S., Shiloh, Y., and Rotman, G. (1995b). The complete sequence of the coding region of the ATM gene reveals similarity to cell cycle regulators in different species. Hum. Mol. Genet. *4*, 2025–2532.

Shafman, T., Khanna, K.K., Kedar, P., Spring, K., Kozlov, S., Yen, T., Hobson, K., Gatei, M., Zhang, N., Watters, D., Egerton, M., Shiloh, Y., Kharbanda, S., Kufe, D., and Lavin, M.F. (1997). Interaction between ATM protein and c-Abl in response to DNA damage. Nature *387*, 520–523.

Shiloh, Y. (1997). Ataxia-telangiectasia and the Nijmegen breakage syndrome: related disorders but genes apart. Annu. Rev. Genet. *31*, 635–662.

Siede, W., Allen, J.B., Elledge, S.J., and Friedberg, E.C. (1996). The *Saccharomyces cerevisiae* MEC1 gene, which encodes a homolog of the human ATM gene product, is required for G1 arrest following radiation treatment. J. Bacteriol. *178*, 5841–5843.

Sikpi, M.O., Wang, Y., and Mallya, S.M. (1998). Defective modulation of double-strand break repair in ataxia telangiectasia cells by gamma radiation. Radiat. Res. *150*, 627–635.

Smilenov, L.B., Morgan, S.E., Mellado, W., Sawant, S.G., Kastan, M.B., and Pandita, T.K. (1997). Influence of ATM function on telomere metabolism. Oncogene *15*, 2659–2665.

Sprung, C.N., Bryan, T.M., Reddel, R.R., and Murnane, J.P. (1997). Normal telomere maintenance in immortal ataxia telangiectasia cell lines. Mutat. Res. *379*, 177–184.

Sugimoto, K., Ando, S., Shimomura, T., and Matsumoto, K. (1997). Rfc5, a replication factor C component, is required for regulation of Rad53 protein kinase in the yeast checkpoint pathway. Mol. Cell. Biol. *17*, 5905–5914.

Sun, Z., Fay, D.S., Marini, F., Foiani, M., and Stern, D.F. (1996). Spk1/Rad53 is regulated by Mec1-dependent protein phosphorylation in DNA replication and damage checkpoint pathways. Genes Dev. *10*, 395–406.

Takagi, M., Delia, D., Chessa, L., Iwata, S., Shigeta, T., Kanke, Y., Goi, K., Asada, M., Eguchi, M., Kodama, C., and Mizutani, S. (1998). Defective control of apoptosis, radiosensitivity, and spindle checkpoint in ataxia telangiectasia. Cancer Res. *58*, 4923–4929.

Taylor, A.M., Byrd, P.J., McConville, C.M., and Thacker, S. (1994). Genetic and cellular features of ataxia telangiectasia. Int. J. Radiat. Biol. *65*, 65–70.

Uhrhammer, N., Fritz, E., Boyden, L., and Meyn, M.S. (1999). Human fibroblasts transfected with an *ATM* antisense vector respond abnormally to ionizing radiation. Int. J. Mol. Med. *4*, 43–47.

Vaziri, H., West, M.D., Allsopp, R.C., Davison, T.S., Wu, Y.S., Arrowsmith, C.H., Poirier, G.G., and Benchimol, S. (1997). ATM-dependent telomere loss in aging human diploid fibroblasts and DNA damage lead to the post-translational activation of p53 protein involving poly(ADP-ribose) polymerase. EMBO J. *16*, 6018–6033.

Vialard, J.E., Gilbert, C.S., Green, C.M., and Lowndes, N.F. (1998). The budding yeast Rad9 checkpoint protein is subjected to Mec1/Tel1-dependent hyperphosphorylation and interacts with Rad53 after DNA damage. EMBO J. *17*, 5679–5688.

Watters, D., Khanna, K.K., Beamish, H., Birrell, G., Spring, K., Kedar, P., Gatei, M., Stenzel, D., Hobson, K., Kozlov, S., Zhang, N., Farrell, A., Ramsay, J., Gatti, R., and Lavin, M. (1997). Cellular localization of the ataxia-telangiectasia (ATM) gene product and discrimination between mutated and normal forms. Oncogene *14*, 1911–1921.

Xia, S.J., Shammas, M.A., and Shmookler Reis, R.J. (1996). Reduced telomere length in ataxia-telangiectasia fibroblasts. Mutat. Res. *364*, 1–11.

Yuan, Z.M., Huang, Y., Ishiko, T., Nakada, S., Utsugisawa, T., Kharbanda, S., Wang, R., Sung, P., Shinohara, A., Weichselbaum, R., and Kufe, D. (1998). Regulation of Rad51 function by c-Abl in response to DNA damage. J. Biol. Chem. *273*, 3799–3802.

Zhang, N., Chen, P., Khanna, K.K., Scott, S., Gatei, M., Kozlov, S., Watters, D., Spring, K., Yen, T., and Lavin, M.F. (1997). Isolation of full-length ATM cDNA and correction of the ataxia-telangiectasia cellular phenotype. Proc. Natl. Acad. Sci. USA *94*, 8021–8026.

Ziv, Y., Bar-Shira, A., Pecker, I., Russell, P., Jorgensen, T.J., Tsarfati, I., and Shiloh, Y. (1997). Recombinant ATM protein complements the cellular A-T phenotype. Oncogene *15*, 159–167.